1. Results

1.1. Virtual Prototyping of Cell Signals

During the course of this thesis, numerical simulations for the microchannel have been carried out. On the one side, a simulation about the shape of a giant magneto resistance (GMR)-sensor signal of cells was performed, where the magnetic momentum was conveyed through magnetic nanoparticles (MNPs) bound to their surface. On the other side, cell aggregates have been looked at in the same manner with different angles respective to the sensor. Both simulations were then correlated to a reference dipole, with the equivalent magnetic momentum distributed in the center of mass.
Additionally, the flow and shear field inside the channel was simulated numerically for the channel cross section as well as for a particle near the walls. A force equilibrium simulation was also established in a basic manner.
Every simulation was captured in a MATLAB class “MRCyte”, which contains material parameters and constants for all simulations above.

1.1.1. Numerical investigation of immunomagnetic label density and size on quantitative magnetoresistive sensing of single cells and cell aggregates

In order to mimic a immunomagnetically labeled cell flowing over the sensor half bridge, the planar integral of the respective magnetic flux density ($\mathbf{B}$) was solved analytically. Here, $\mathbf{r}_i$ specifies the distance vector of a single MNP from the sensor plane. The magnetic flux density was converted by the GMR to a resistive change $\mathbf{R}_{sig}$ by scaling it with the GMR-sensitivity S and subsequently into a signal voltage $\mathbf{V}_{sig}$ inside the bridge branch.(Eq. 1.1 and **????**)
In the numerical approach, MNPs were randomly sampled on a sphere surface with an equivalent diameter of 4 µm or 8 µm. Then, the signal was computed for every MNP during every timestep. Additionally, the MNP distribution was rotated in every iteration to resemble a rolling motion. The computed signals were then cross-correlated to the signal of a reference flux density $\mathbf{B}_{ref}$ caused by a point-like magnetic moment located in the geometric center of the same sphere.

$$\mathbf{B}(t) = \sum_{i=1}^{N} \frac{1}{A_{\text{Sensor}}} \int_{-\frac{l}{2}}^{\frac{l}{2}} \int_{-\frac{w}{2}}^{\frac{w}{2}} \frac{\mu_o}{4\pi} \left(\frac{3\mathbf{r}_i(t)\,(\mathbf{r}_i(t) * \mathbf{m}_i)}{|\mathbf{r}_i(t)|^5} - \frac{\mathbf{m}_i}{|\mathbf{r}_i(t)|^3} \right) dxdy \qquad 1.1$$

$$\mathbf{R}_{sig}(t) = -\mathbf{B}(t) * \frac{S}{100} * R + R \qquad 1.2$$

$$\mathbf{V}_{sig}(t) = \frac{\mathbf{R}_{sig}(t)}{R + \mathbf{R}_{sig}(t)} * V_p - \frac{V_p}{2} \qquad 1.3$$

By its formula, cross-correlation $R_{xy}(\tau)$ yields a displacement dependent signal through its convolution of the complex conjugated reference signal $\mathrm{V}^*_{ref}(t)$ with the sample signal $\mathbf{V}_{sig}(t+\tau)$.(Eq. 1.4) Therefor, only the maximal correlation of this function was considered in further analyses.

$$\max\{R_{xy}(\tau)\} = \max\left\{\int_{-\infty}^{\infty} \mathrm{V}^*_{ref}(t)\mathbf{V}_{sig}(t+\tau)dt\right\} \qquad 1.4$$

gnal Similarity
r Cells With
rying Bead
verages,Cross-
rrelation
tween single
ole with
m magentic
ment and
face covered
h randomly
tributed mag-
tic particles,
nulation of cell
ling velocity
d forces

1.1.2. Single Cell Signal

Aim of these simulations is to find a measure of how magnetic labelling of a cell affects signal shape and its subsequent analysis. A single cell with a surface coverage of 5 % to 99 % of a densely packed sphere was loaded randomly with MNPs at different sizes. As shown in the schematic Fig. 1a, not only signal peak amplitude but also full width at half maximum (FWHM) increases at growing coverages.

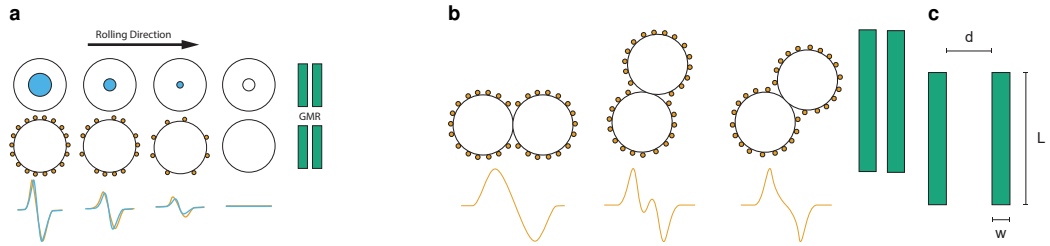

Figure 1: Particle Coverage Simulation
(**a**) The single ideal magnetic dipole in the center (●) causes a signal deviation from the real cell signal with magnetic moment distributed on the cell surface (●) (**b**) Signal shapes of different angles of 2-particle aggregates (**c**) GMR Sensor simulation dimensions

simulation Parameters

why the cell signal differs –> number of aggregates –> single particle moments are more weighted

PArticle size is dependent –> number less, but moment higher –> single particle is even more important

1.1.3. Cell Aggregates

1.2. Reference Bead Surface Functionalization

1.2.1. Amine-Surface Biotinylation

Streptavidin-Atto488 reference calibration Anti-Biotin-PE working? BNF-Dextran-Streptavidin unspecific binding?

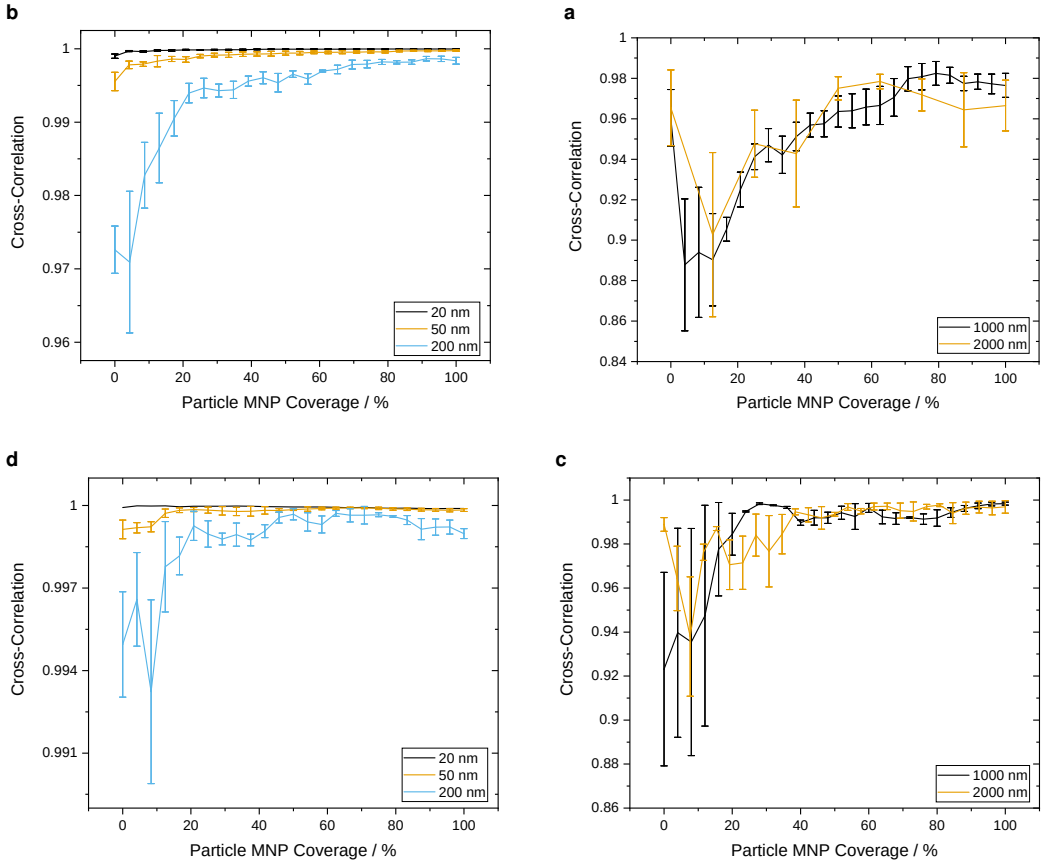

Figure 2: Coverage Dependent Signal Correlation
Mean from 3 differently distributed particles, SEM (**a**) d = 4 µm (**b**) d = 4 µm (**c**) d = 8 µm (**d**) d = 8 µm

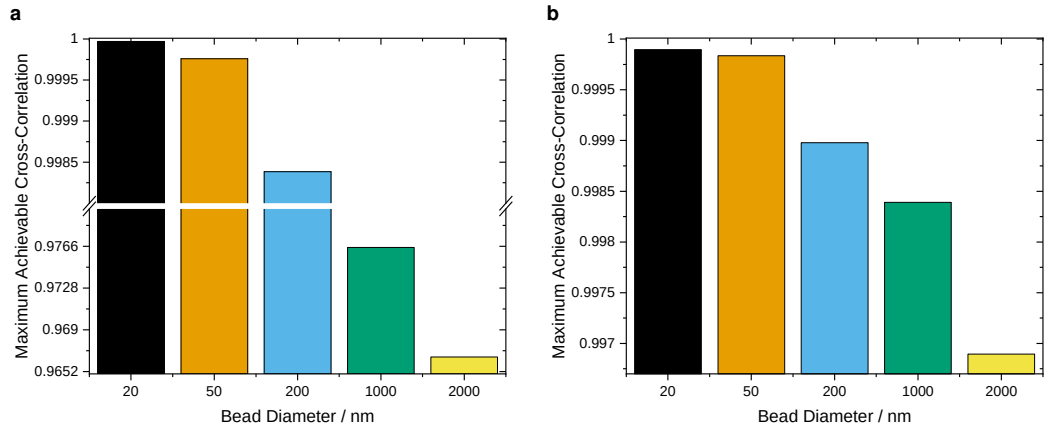

Figure 3: Difference of Cross-Correlation at Maximum Coverage
Mean from 3 different particle distributions at maximum coverage(**a**) d = 4 µm (**b**) d = 8 µm

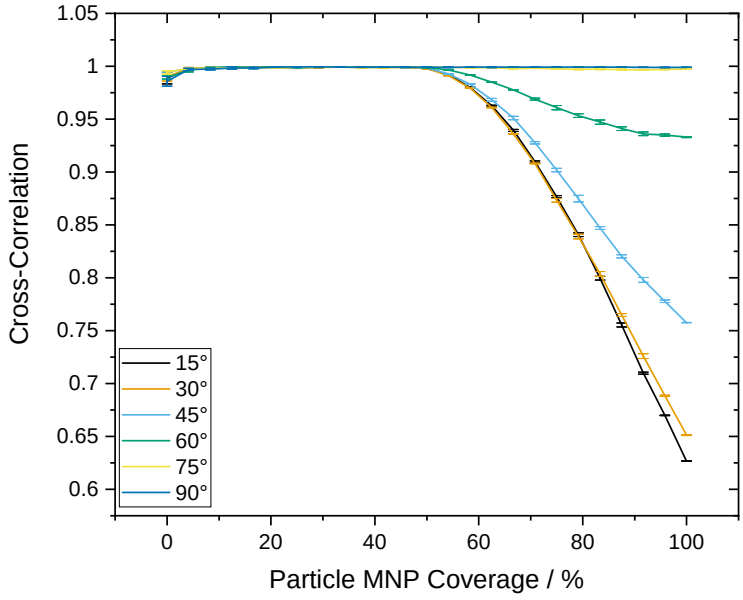

Figure 4: Sensor Signals Correlation between Two Cell Aggregates At Shifting Angles with a Reference Dipole
Mean from 3 differently distributed particles, SEM

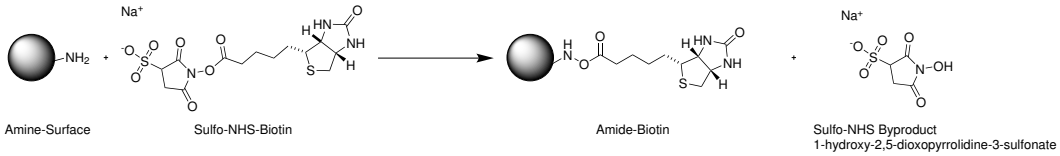

Figure 5: Amine Bead Modification with Sulfo-NHS-Biotin
An amine terminated bead is incubated with sulfo-NHS-Biotin to cover its surface by amide-Biotin. As byproduct the sulfo-NHS-ester 1-hydroxy-2,5-dioxopyrrolidine-3-sulfonate splits off.

1.3. Concentration Measurements in MRCyte

Explain v-c

1.3.1. Calibration of Flow Field
1.3.2. Count Stability
Measurement over 1h

Concentration Measurement in Diluted Whole Blood
1.3.3. Differential Counting Setup
Sensitivity Calibration
Concentration Measurement in Buffer Solution
1.3.4. Surface Magnetization of Biofunctionalized Beads
Somehow BNF-Dextran showed unspeficity initally, but not anymore later on

1.4. Surface Modification and Biofunctionalization of the Sensor Chip Substrate

1.4.1. Physisorption
Quantification in Plate Reader Trial with Neutravidin + Sensor (Esthis Versuch)

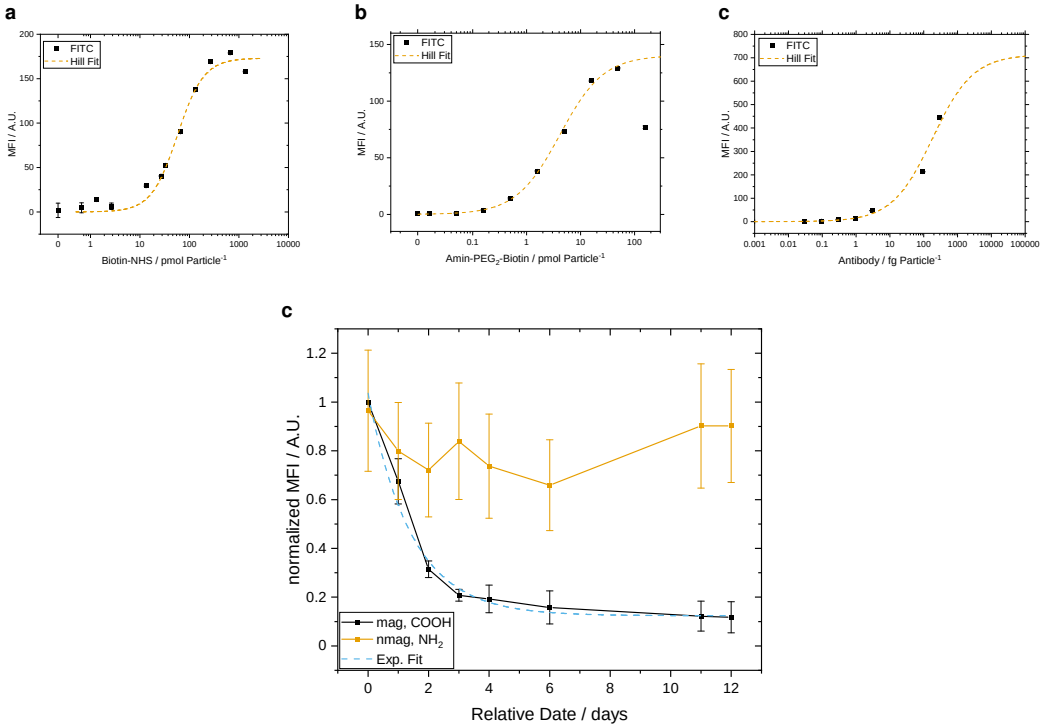

Figure 6: Titration of Biofunctional Molecules on 8 µm Particles
(**a**) NHS-Biotin, MFI, CV, reduced chi square = 275.19597, Hill Fit $y = Vmax * x^n/(k^n + x^n)$, Vmax = 173.077, k = 0.0572831, n = 1.63554 (**b**) Amin-PEG$_2$-Biotin MFI, CV, outlier neglected Gleichung: $y = Vmax * x^n/(k^n + x^n)$ Vmax 171,02602, k 0,04201, n 0,91338,Chi-Quadr Reduziert 4,07387 (**c**) MFI, CV, reduced chi square = 0.91011, Hill Fit $y = Vmax * x^n/(k^n + x^n)$, Vmax = 713.83643, k = 182.83011 , n = 0.72458 (**d**) MFI, SEM, τ_{decay} = 1.425 57 ± 0.161 88 Equation $y = A \exp^{\frac{-x}{\tau_{decay}}} + y_0$ y0 0.12369 ± 0.01576 A1 0.91263 ± 0.06964 t1 1.42557 ± 0.16188 Reduced Chi-Sqr 0.00542

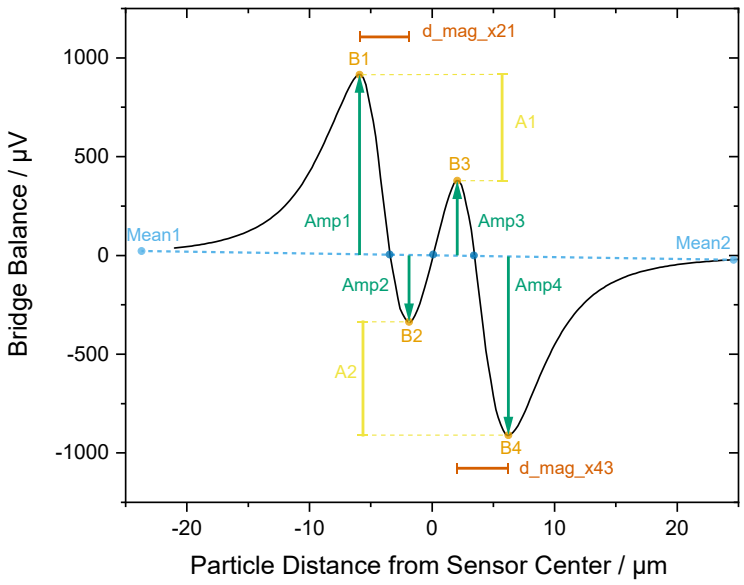

Figure 7: Example Signal of Magnetic Measurement
explain all

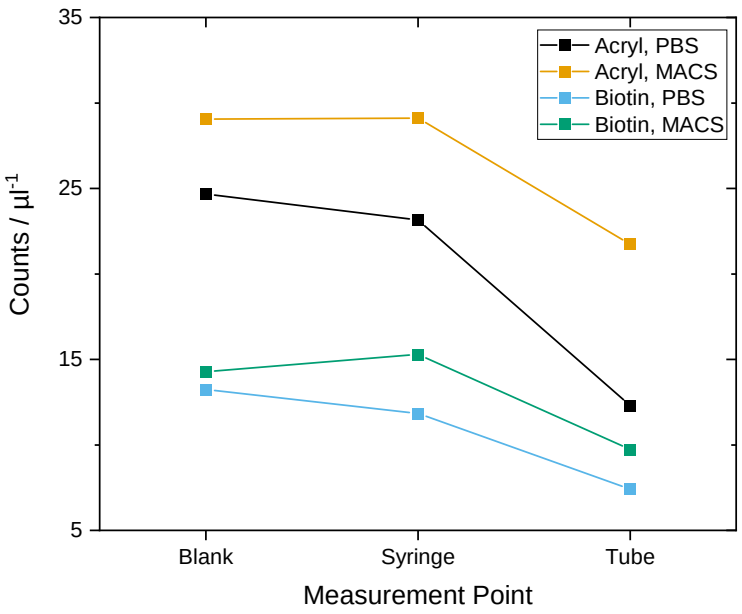

Figure 8: Bead Loss Evaluation in Connectors
Losses in different buffers and bead surfaces.

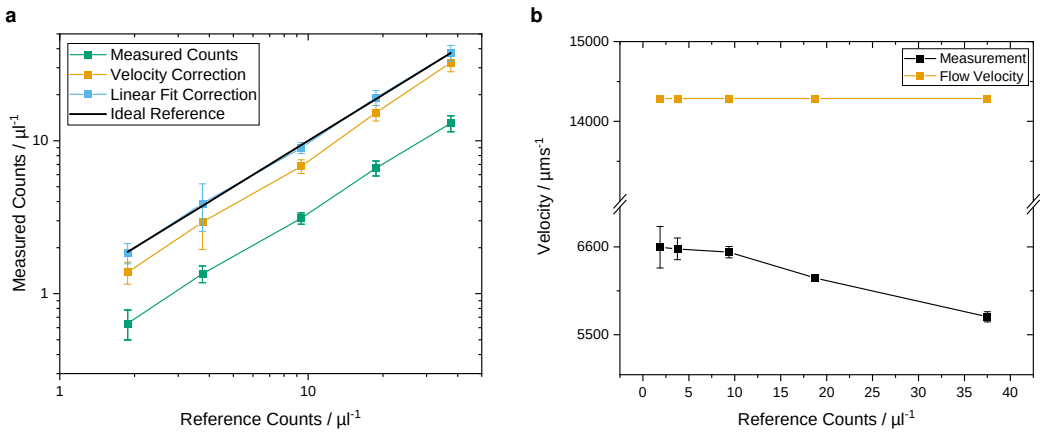

Figure 9: Absolute Concentration Measurements
Mean from 3 independent measurements(**a**) mean, sd (**b**) mean, SEM, Reference Count based error: Liner fit steepness 0.346 22 $\pm$ 0.009 68 –> Correction Factor (inverse) 2.888 33 $\pm$ 0.080 75, Velocity Based Correction: Q/A Dims: 700 µmx50 µm Q = 30 µL min^{-1} –> 2.261 09

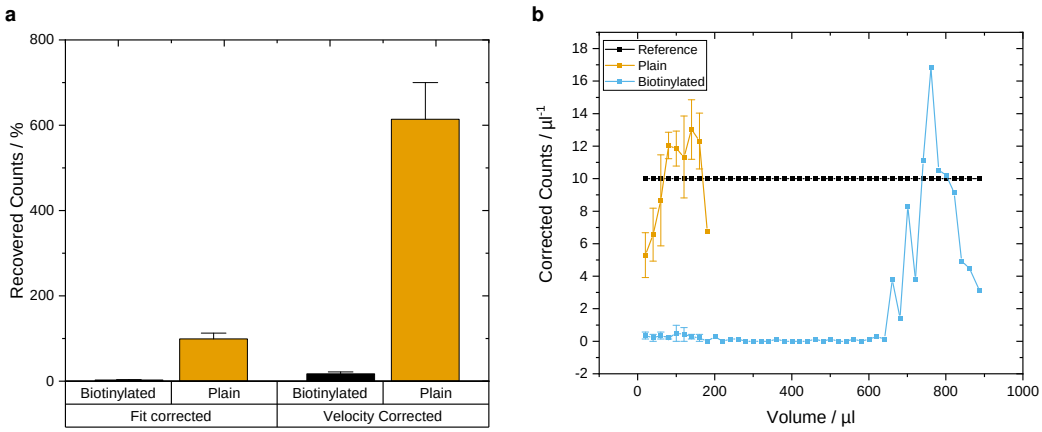

Figure 10: Error Sources in Concentration Measurements
(**a**) mean, SEM Fit factor comparison with protein coated surfaces (**b**) mean, SEM

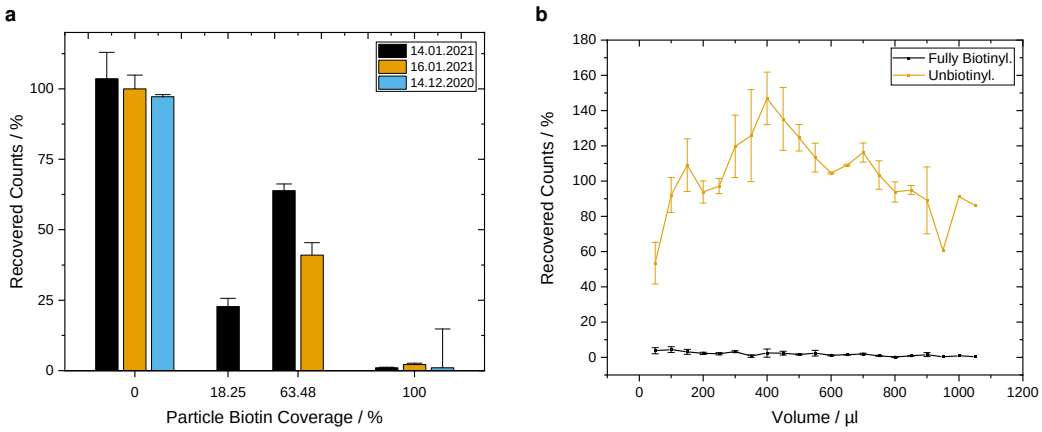

Figure 11: Reproducibility of Concentration Measurements with Saturated Neutravidin Surface
(**a**) 80 µL min^{-1} mean, SEM (**b**) All,mean, SEM,

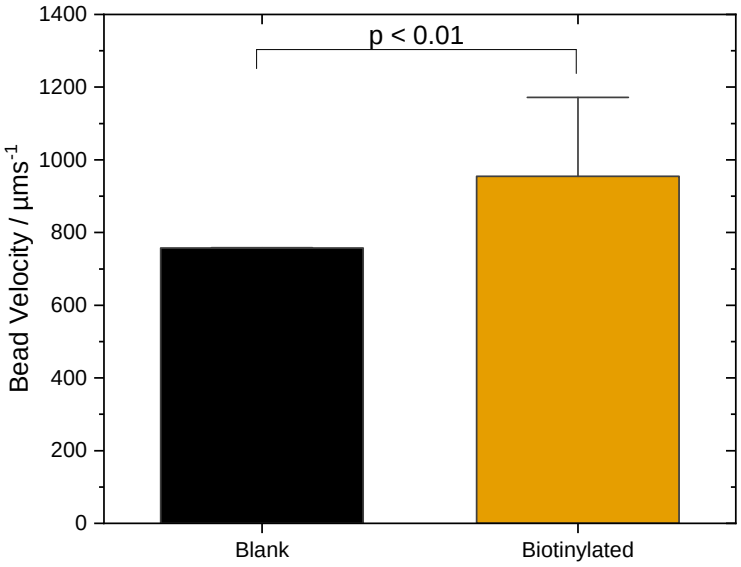

Figure 12: Measured Bead Velocity
p < 0.01

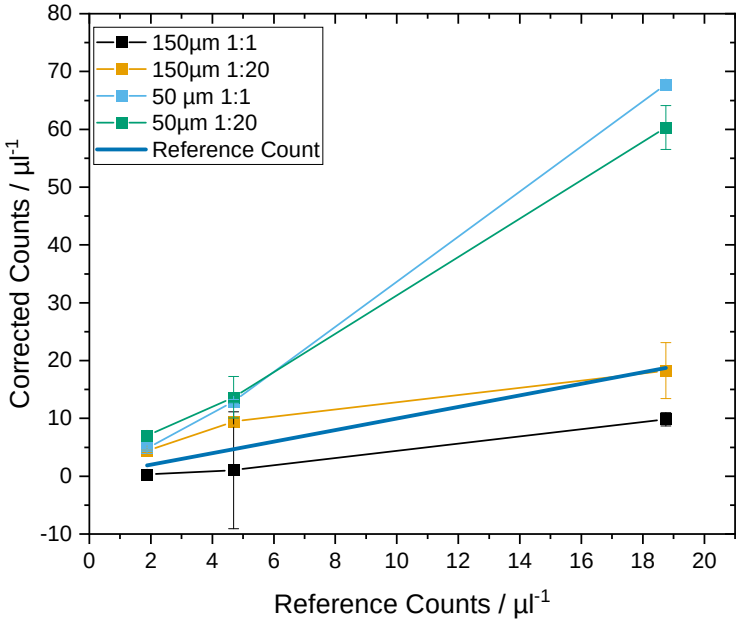

Figure 13: Absolute Concentration Measurement in Blood Samples Under Varying Channel Height
Velocity Correction does not work for high concentrations in 50 µm

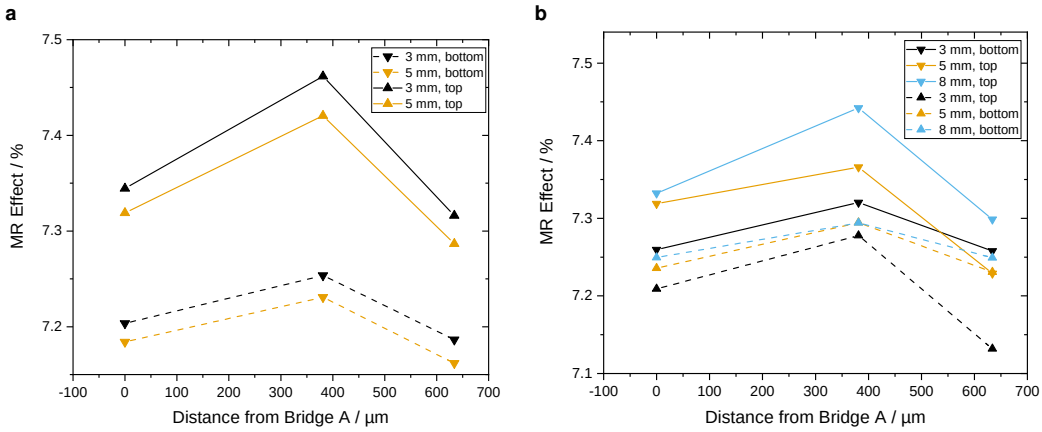

Figure 14: Hysteresis Calibration for Stacked Printed circuit board (PCB)
(**a**) Optimized for top sensor (**b**) Optimized for bottom sensor

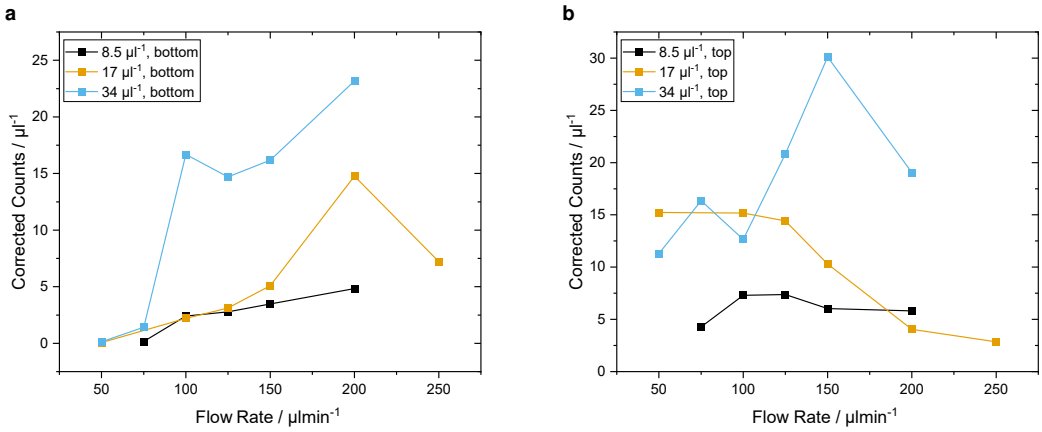

Figure 15: Flow Rate Dependency of Counting Setup
(**a**) Optimized for top sensor (**b**) Optimized for bottom sensor

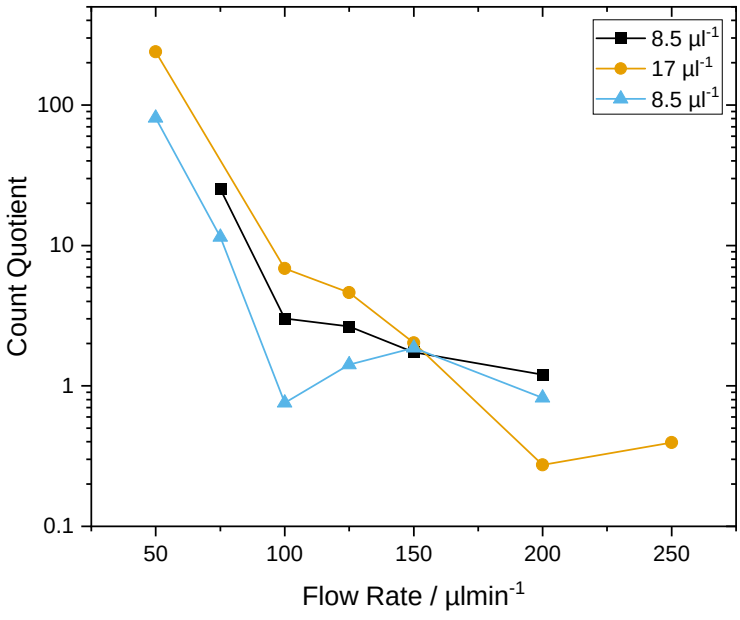

Figure 16: Optimal Differential Counting Flow Rate
Losses in different buffers and bead surfaces.

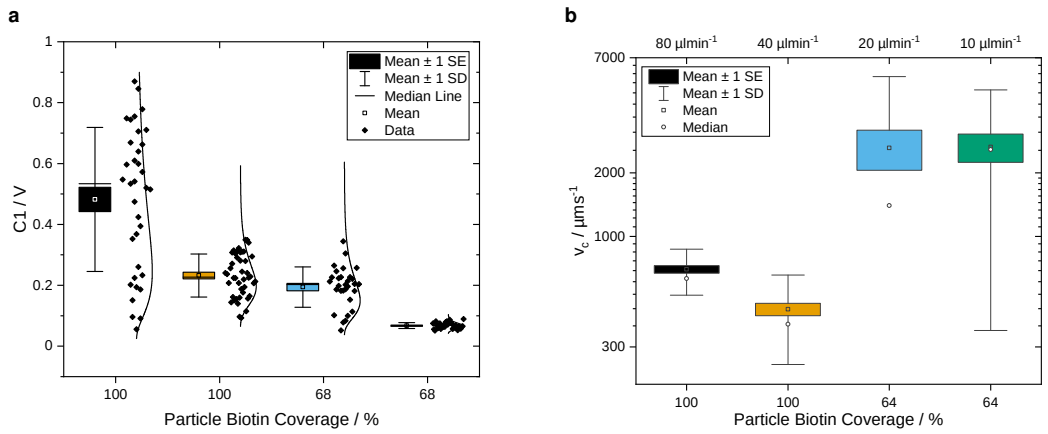

Figure 17: Bead Coverage Assay with BNF-Dextran-redF-100 nm
(**a**) 1. 80 µL min^{-1} 2. 40 µL min^{-1} 3. 20 µL min^{-1} 4. 10 µL min^{-1} (**b**) d = 8 µm

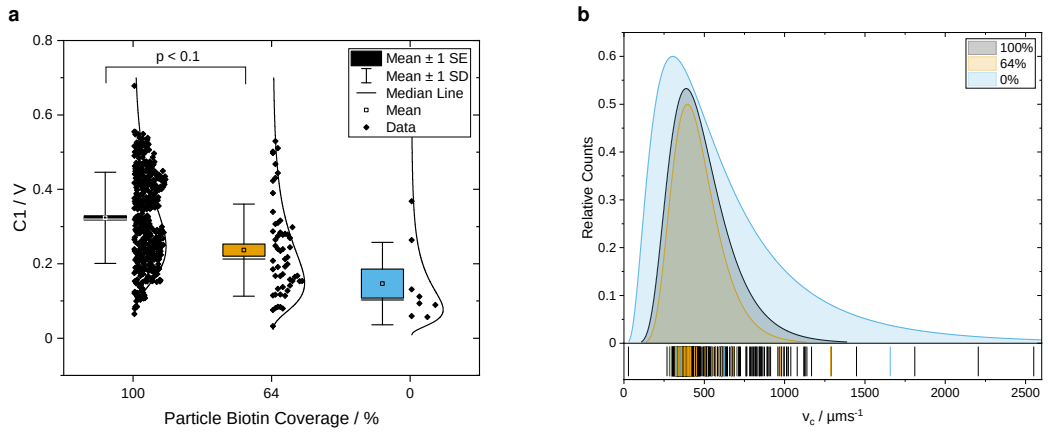

Figure 18: Bead Coverage Assay with OceanNanotec 50 nm
Mean from 3 different particle distributions at maximum coverage, SEM(**a**) d = 4 µm (**b**) d = 8 µm

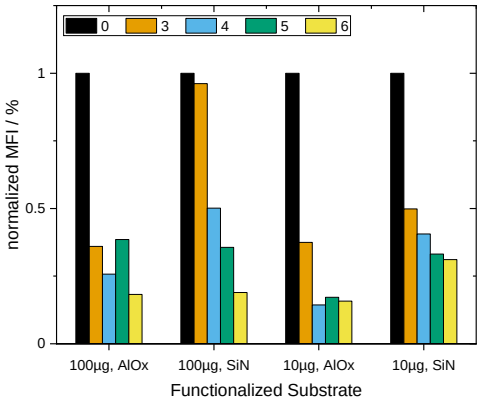

Figure 19: Surface Adsorption Stability of Neutravidin on Silicon nitride (Si_3N_4) and Aluminium oxide (Al_2Ox_3)
Blank with PBS and Blank substrate, corrected, then normalized, absolute protein per ~25 mm

1.4.2. Covalent Attachment

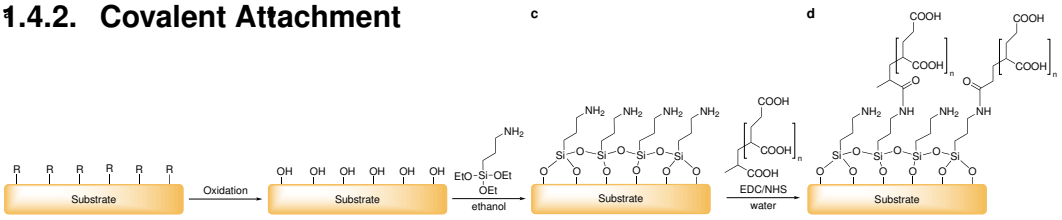

Figure 20: General process chain of chemical surface modification
Any substrate with various surface groups R (**a**) is oxidized to exhibit −OH (hydroxyl) groups.(**b**). Then a silane self-assembled monolayer (SAM) is attached (**c**) and subsequently modified by carbodiimide chemistry with Poly(acrylic) Acid (PAA). (**d**)

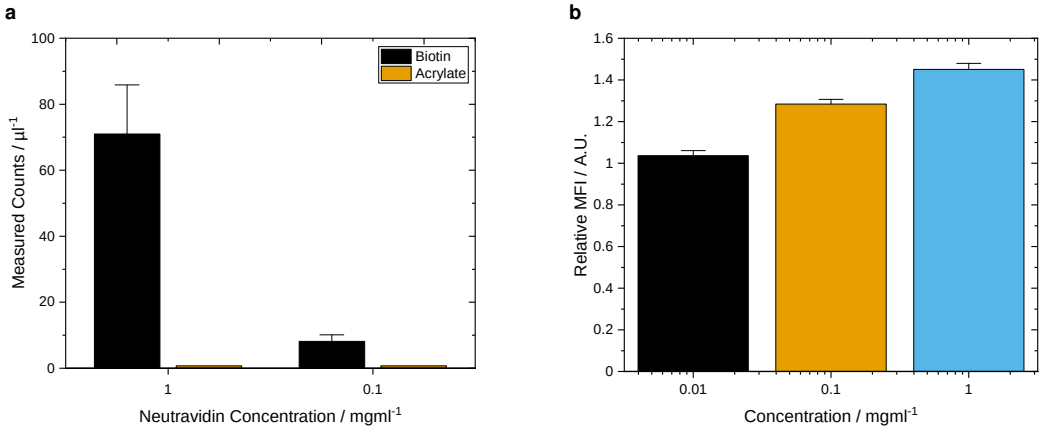

Figure 21: Neutravidin Titration Fluorescence and Bead Capture Assay
Relate count to area, then change MFI to counts μL^{-1} mm^{-2}(**a**) Serpentine (**b**) Glass

Plasma-Based Approach
Water-Based Approach

Sonicate in Acetone and Water 5' 1:1 hydrochloric acid (HCl):Methanol sulfuric acid (H_2SO_4) Treat for 30 min in light boiling water

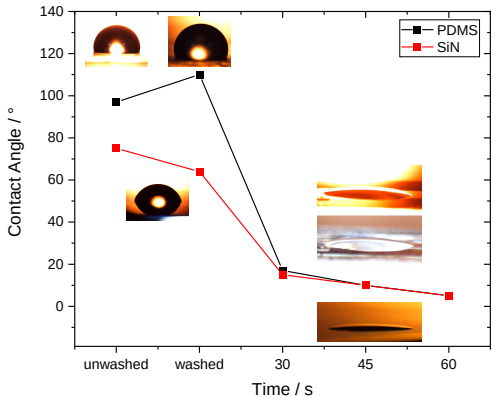

Figure 22: Hydrophbicity Analysis of poly(dimethyl siloxane) (PDMS) under Plasma Exposure
test123